Desalination and Water Treatment
www.deswater.com
doi: 10.1080/19443994.2012.749052

51 (2013) 2592–2601
March

Taylor & Francis
Taylor & Francis Group

Effect of surface modification of activated carbon on its adsorption capacity for bromate

Li Gu[a,b], Dandan Wang[a,b], Rui Deng[c], Hongxia Liu[a,b,*], Hainan Ai[a,b]

[a]*Institute of Urban Construction And Environmental Engineering, Chongqing University, 174 Shapingba Road, Chongqing 400045, P.R. China*
Tel./Fax: +86 65120980; email: guli@cqu.edu.cn
[b]*Key Laboratory of the Three Gorges Reservoir Region's Eco-Environment, Chongqing University, Ministry of Education, 174 Shapingba Road, Chongqing 400045, P.R. China*
[c]*College of River and Ocean Engineering, Chongqing Jiaotong University, 66 Xuefu Road, Chongqing 400074, P.R. China*

Received 21 November 2011; Accepted 9 September 2012

ABSTRACT

This study deals with bromate adsorption by using modified activated carbons (ACs), attempting to reveal the effect of different modification methods on bromate adsorption by performing kinetic and isotherm tests. Four carbon modification methods including thermal modification, HNO_3 modification, H_2O_2 modification, and NaOH modification are applied. These modification methods change the porous structures and redistribute the surface functional groups of AC. The kinetic data have been analyzed using pseudo-second-order and intra-particle diffusion models, and the intra-particle diffusion model is found to be the best applicable model to describe the adsorption process. The isothermal test shows that the thermal and alkaline modified ACs, with lower acidic functional groups, present higher adsorption capacities, and there is a remarkable linear relationship between the maximum adsorption capacity and the proportion of the acidic groups. The presence of natural organic matters (NOM) lowers the capacities of these ACs in bromate adsorption, but the HNO_3 modified AC was not as sensitive as other modified samples. The presence of other anions (NO_3^-, SO_4^{2-}, Cl^-) can reduce the bromate uptake and the selectivity order for the AC is $NO_3^- > SO_4^{2-} > Cl^-$.

Keywords: Bromate; Activated carbon; Adsorption; Modification

1. Introduction

Bromide (Br^-) is commonly found in source water. In disinfection processes of water production, it can be oxidized to bromate (BrO_3^-) during its interactions with molecular ozone (O_3) and hydroxyl radical ($HO\cdot$) [1,2]. Recently, bromate in drinking water has received great concern due to its toxicity. It has been classified by USEPA as a carcinogenic substance to humans by oral route of exposure. A maximum contaminant level of 10 μg/l has been set by WHO, European Commission and USEPA [3]. Consequently, it is of great importance to pursue methods to remove bromate from water.

A large number of chemical and physical methods have been suggested to remove bromate from water.

*Corresponding author.

These methods include reduction (zero-valent iron (Fe^0) or Fe^{2+} reduction) [4–7], Reverse osmosis filtration [8–10], ionic exchange [11,12], UV irradiation [13–15] etc. Previous studies have proved that these methods are efficient in bromate removal. However, due to their high operational costs and complicated procedure in treatment, the commercial-scale applicability of these methods is limited. Comparatively, the processes based on adsorption seem to be more attractive due to their simplicity in design and operation.

Activated carbon (AC, granular or powder), as an outstanding adsorbent, has been widely applied in removing pollutants from water [16,11,17]. It is also applied in bromate removal due to the fact that the AC surface possesses ion-exchange property and can form chemical bonds with ions. Previous studies show that some adsorbents such as Nano-Al_2O_3, corncobs [18,19], and AC are suitable in the removal of bromate from water. The capacity of the ACs is carbon-specific and depends on the source water [3,20,21]. Mechanism of bromate removal in AC adsorption has also been postulated. The process is regarded to be adsorbed, reduced to hypobromite (BrO^-) and finally reduced to bromide (Br^-) on AC surface. Following reactions show that the reduction processes occur during bromate adsorption [3,13,22].

$$\equiv C + BrO_3^- \rightarrow BrO^- + \equiv CO_2 \quad (1)$$

$$\equiv C + 2BrO^- \rightarrow 2Br^- + \equiv CO_2 \quad (2)$$

It is commonly acknowledged that the adsorption capacity of the AC depends on its porous structures and the functional groups on the surface. So, according to the postulated reduction mechanism, it can be speculated that the capacity of AC on bromate adsorption strongly depends on the surface conditions and the properties of the AC. During past decades, efforts have been done to test the effect of surface porosity and functional properties on bromate adsorption. Previous studies have revealed that the acidic oxygen groups created in AC oxidation can block the adsorption or reduction sites [19,23]. Increase of the amount of oxygen groups on the AC surface can bring an increase in the acidity of AC and makes the surface negatively charged. Under the unfavorable electrostatic interactions between the bromate anions and the acidic groups, the adsorption of bromate tends to be reduced. It is also reported that the ACs with less surface oxygen present better anion exchange capacity due to its positive charge on the surface [3,19]. Several reduction modification methods such as thermal and basic modification could reduce the amount of oxygen on the AC surface [24,25], and further increase the capacity in bromate removal. However, though the methods of AC modification have been widely studied, comprehensive studies about the effect of these modification methods on the bromate adsorption capacity of the AC, as well as the relationship between surface functional groups and the adsorption capacities are rarely found. Furthermore, works about some important indexes such as adsorption kinetics, isotherm and maximum adsorption capacity for optimization selection of AC to remove bromate are still limited.

Purpose of this study is to reveal the effects of different modification processes on the bromate adsorption of the AC. Four types of modification processes including thermal modification, HNO_3 modification, H_2O_2 modification, and NaOH modification are applied. These modified ACs are characterized and the adsorption isotherm, as well as the kinetics of these ACs are evaluated and compared. In addition, the relationship between surface functional groups and adsorption capacities is revealed and the mechanism of bromate adsorption is developed.

2. Materials and methods

2.1. Chemicals and materials

AC was purchased in YiXin industrial Co., China. These AC were crushed and screened and those with particle size of 1–2 mm were selected. Prior to modification, they were washed and dried. Bromate working solution was prepared using bromate stock solution (1.0 g/l), which is prepared by dissolving $KBrO_3$ (Sinopharm Chemical Reagent Co. Ltd, China) into deionized water.

2.2. Preparation of modified ACs

The ACs were oxidized with different concentrated solutions such as HNO_3 (20 g AC in 200 ml 5% HNO_3) and H_2O_2 (20 g AC in 200 ml 5% H_2O_2) at 60°C for 2 h and then were washed several times in deionized water and dried at 105°C. These modified ACs are named as AC-A and AC-O, respectively. The alkali modified AC (AC-B) was prepared in NaOH solution (20 g AC in 200 ml 2% NaOH) at 25°C for 4 h. In addition, thermal-treated AC sample, named as AC-H, treated in N_2 atmosphere at 550°C was also applied to make a comparison.

2.3. Adsorption experiments

Standard adsorption equilibrium experiments ("bottle point") were applied to evaluate the capacity

Table 1
Textural property of modified AC samples

	S_{BET} (m^2/g)	R_p (nm)	V_{meso} (cm^3/g)	V_{micro} (cm^3/g)	V_p (cm^3/g)	S_{micro} (m^2/g)	S_{micro}/S_{BET}
Virgin AC	654	2.33	0.09	0.31	0.40	591	0.90
AC-H	643	2.33	0.09	0.28	0.37	596	0.93
AC-A	489	2.47	0.11	0.19	0.30	408	0.83
AC-B	554	2.35	0.09	0.24	0.33	480	0.87
AC-O	548	2.38	0.10	0.23	0.33	465	0.85

of the ACs in bromate removal. Working solutions of 200 ml (in flask) at different concentrations of the bromate were prepared. After addition of certain quantities (about 200 mg) of the ACs, these flasks were shaken at 25°C for 48 h. After the adsorption process attained equilibrium, the solutions were taken for analysis. The pH of the solution was maintained at a defined value (6.0 ± 0.02) by buffer solutions. Before analysis, the sample was filtrated through 0.45 μm pore-sized membrane.

Bromate adsorption kinetics was evaluated for all the modified ACs. Before the start of each kinetic experiment, approximately 0.2 g of the sample was loaded in a 250 ml conical flask. Then, 200 mL of the bromated solution (60 mg/l) was added. The flask was capped and immersed in a thermostatic shaker bath at 25°C and 200 rpm. The pH of the solution was maintained at 6.0 ± 0.02. Then, the reaction solution was taken out at different time intervals from 0 to 24 h of adsorption.

In equilibrium experimental section, a series of suspensions in conical flask were prepared, each containing 0.25 g of samples and 200 ml bromate solution. These solutions had different bromate concentrations in the range of 0–200 mg/l. Each flask was capped and shaken for 48 h.

2.4. Analysis

The concentration of the bromate was analyzed by ion chromatography (DIONEX, ICS-3000, USA). The bromate was separated by mobile phase of 45 mM potassium hydroxide (KOH) delivered at the flow rate of 1.2 ml/min. A 50 μl sample was injected. The separation column was DIONIX IonPacAS23 (4.0 × 250 mm). Suppressed conductivity detector was maintained at 35 ± 0.1°C. The bromate concentrations were measured twice and the mean values were applied.

The AC samples were characterized by using nitrogen adsorption–desorption method by using BELSORP-mini surface area analyzer. BET surface area, average pore radius (R_p), and total pore volume (V_P) were obtained from the adsorption–desorption isotherms. The total pore volume was evaluated directly from the nitrogen isotherm when the volume of N_2 (as liquid) was held at $P/P_0 = 0.99$. The *t*-plot method was applied to determine the micropore volume (V_{micro}).

pH_{PZC} (point of zero charge) was determined by mass titration, which was previously described by Noh and Schwarz [26]. A 100 ml volume solution of different initial pH and various amounts of carbon samples (0.1, 0.5, 1.0, 5, 10, 15, and 20%) were added to 250 ml Erlenmeyer flasks. The equilibrium pH value which the mixture approached asymptotically with increasing AC concentration was taken as the pH_{PZC}.

Surface functional group was analyzed by using the method established by Boehm [27]. The AC sample was added into different solutions (0.05 N $NaHCO_3$, Na_2CO_3, NaOH or HCl), respectively. These samples were mixed continuously at 25°C for 24 h. A certain volume of supernatant was taken from the above mixtures and back titrated with HCl (or NaOH) (0.05 N) solution. The compositions of surface functional groups were determined by the residual basicity (or acidity) through back titration.

3. Results and discussion

3.1. Characterization of the ACs

3.1.1. Texture properties

Nitrogen adsorption–desorption process is conducted for all of these AC samples. All of the adsorption isotherms can be categorized as type I of the IUPAC classification (typical microporous adsorbent). Textual properties such as average pore radius (R_p), pore volume (V_p), mesoporous volume (V_{meso}), and microporous volume (V_{micro}) calculated from the N_2 isotherms of the AC samples are summarized in Table 1.

The BET surface area (S_{BET}) of the virgin AC is about 654 m^2/g with the area of micropore (S_{micro}) of 591 m^2/g. The thermal modification process hardly changes the porous structure of the AC and the S_{BET}

of the AC-H is close to that of the virgin AC. These results are quite different from the previous reports that the thermal treatment can significantly increase the specific surface area (the increase mainly occurs in microporous size) and the total pore volume [25]. In addition, from the figure, S_{micro} of the AC-H is slightly higher than that of the virgin AC. Ratio of S_{micro}/S_{BET} is considered as an important index revealing the porous structure, and it is found that the ratios of the virgin AC and AC-H are about 0.90 and 0.93, respectively. The process of HNO_3 oxidation changed the porous structures of the AC dramatically. From the table, the S_{BET} and S_{micro} of the AC-A decreases to about 489 and 408 m^2/g, while the ratio of S_{micro}/S_{BET} decreases to 0.83. The reductions of these indexes are commonly regarded to have a negative effect on the capacity of the AC in adsorption of some organic pollutants. The H_2O_2 and NaOH modification process also decrease the S_{BET}, V_p, and S_{micro} of the ACs. The S_{BET} of AC-B and AC-O are about 554 and 548 m^2/g, while the S_{micro}/S_{BET} ratios of the two ACs are about 0.87 and 0.85, respectively.

3.1.2. Surface chemical properties

According to Boehm [27], $NaHCO_3$ neutralizes carboxylic acids; Na_2CO_3 neutralizes carboxylic and lactone groups; and NaOH neutralizes carboxylic, lactone, and phenol groups. In addition, the basic groups can be neutralized by HCl. The Boehm results are applied in this study to reveal the changes of surface chemical groups by these modification processes. Table 2 shows the contents of acidic and basic surface functional groups of different AC samples.

It can be seen from the table that the concentrations of the total acidic and basic groups are 0.83 and 0.70 mmol/g, and the pH_{PZC} of the virgin AC is about 6.7. These modification processes redistribute the surface functional groups. In the thermal modification process, the amounts of the carboxylic groups are decreased, corresponding with the slight increase in the amount of the lactone groups. The amount of the basic groups of AC-H is about 0.75 mmol/g, which is slightly higher than that of the virgin AC. The thermal modification process increases the pH_{pzc} slightly from 6.7 to 6.8. These changes found in thermal modification can be ascribed to the decomposition of carboxylic groups under higher temperature.

In HNO_3 modification process, HNO_3 oxidized the unsaturated bonds on AC surface and formed acidic oxygen groups. Thus, higher amount of the carboxylic and lactone groups on the surface of AC-A are found [25,28]. Eqs. (3)–(5) show the possible reaction pathways in HNO_3 modification.

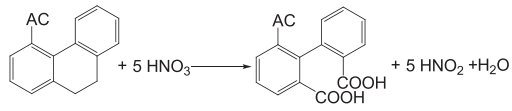

(3)

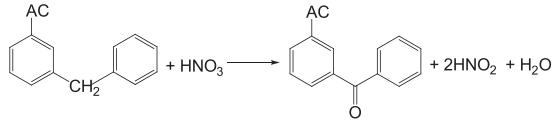

(4)

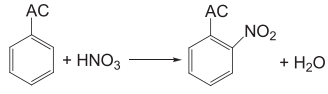

(5)

The acidic groups are formed rapidly during the interactions between HNO_3 and AC particles, and thus, the pH_{PZC} of the AC is decreased significantly to about 3.2. The lowered pH_{PZC} of the sample means that the AC surface is negatively charged at normal pH conditions. Due to the electrostatic repulsion between the bromate anions and the negatively charged surface, the capacity of the AC-A in adsorption of bromate is likely to be reduced.

In H_2O_2 modification, due to the fact that the H_2O_2 has a property of electrophilic attacking, the oxidant attacks the unsaturated bonds of C = C by electrophilic addition and introduces the phenolic groups onto the surface. With the reaction proceeding, the phenolic groups could be further oxidized to bands C=O and –COOH, and finally results in the decrease of the amount of the lactone and phenolic groups. In

Table 2
Surface chemical property of different AC samples

Samples	pH_{PZC}	Surface chemical groups (mmol/g, averaged concentration)				
		Phenolic groups	Lactone groups	Carboxylic groups	Basic groups	Total acidic groups
AC	6.7	0.26	0.12	0.45	0.70	0.83
AC-H	6.8	0.26	0.19	0.33	0.75	0.78
AC-A	3.2	0.27	0.16	0.97	0.22	1.40
AC-B	7.3	0.47	0.07	0.23	0.86	0.77
AC-O	5.9	0.36	0.17	0.57	0.82	1.10

addition, free radicals (such as HOs) are commonly formed and released in H_2O_2 decomposition. These radicals, which are very active in oxidation reactions in aqueous phase, can also oxidize the unsaturated bonds on AC surface, and finally redistribute the surface functional groups [25]. Eqs. (6)–(8) show the reaction pathways in H_2O_2 modification.

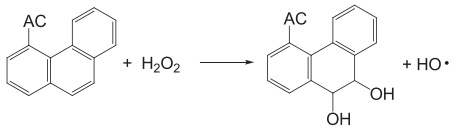

(6)

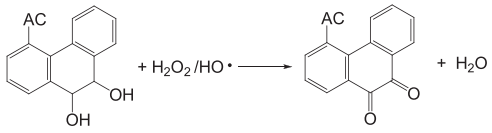

(7)

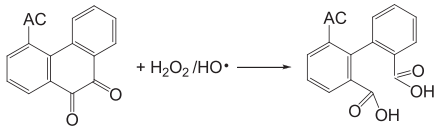

(8)

NaOH treatment increases the pH_{PZC} of the AC to about 7.3. As shown in Table 2, the phenolic group increases from 0.26 to 0.47 mmol/g, the lactone group decreases from 0.12 to 0.07 mmol/g, and the carboxylic group decreases from 0.45 to 0.23 mmol/g. The major change takes place in the phenolic and the carboxylic groups. Tryk proposed the following conceptual scheme of the reaction between NaOH and AC [24]:

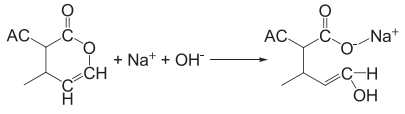

(9)

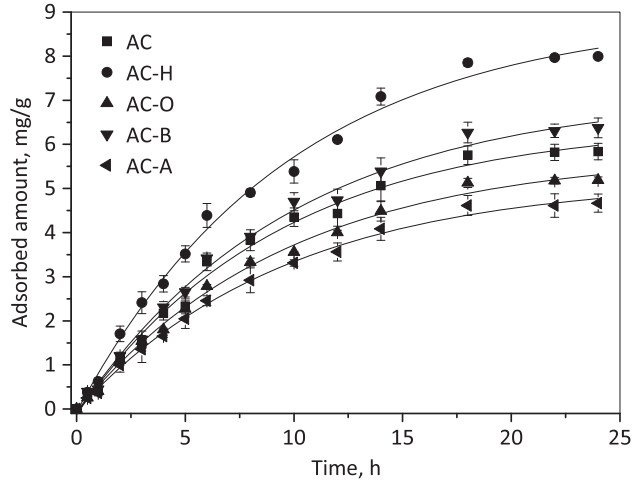

Fig. 1. Experimental kinetic data for bromate adsorption.

3.2. Adsorption kinetics

Kinetic study of adsorption processes provides useful data regarding the efficiency of adsorption and feasibility of scale-up operations. Adsorption kinetic data for different AC samples are shown in Fig. 1. It can be seen from the diagram that the rate of the bromate adsorption by AC is slow. Most amounts of the bromate are captured during the first 12 h of the adsorption, and the equilibrium tends to be established after approximately 18 h of shaking. Also, it can be seen that the sample AC-H presents the highest capacity, while the samples AC-O and AC-A present lower capacities in bromate adsorption at this condition.

For an insight into the reaction process of bromate adsorption by these ACs, two kinetic models are applied. One is pseudo-second-order model; the other is intra-particle diffusion model. Equation of the pseudo-second-order model [29] is shown as following:

$$\frac{dq_t}{dt} = k(q_e - q_t)^2 \tag{10}$$

In the equation shown above, k (g/(h·mg)) is the rate constant while q_t and q_e are the amount of bromate adsorbed at time t and the adsorption equilibrium, respectively. At initiation of the adsorption, $q_t = 0$. So the equations can be integrated to yield:

$$\frac{t}{q_t} = \frac{1}{kq_e^2} + \frac{t}{q_e} \tag{11}$$

The parameters including k and q_e of the equation can be obtained from the intercept and slope of the plot of (t/q_t) vs. t (shown in Fig. 2(a)). Results of the model fitting are also shown in Table 3. The high values of the coefficient shown in the table indicate that the process of bromate adsorption by these ACs can well be described by the pseudo-second-order model. The rate constants k for virgin AC, AC-H, AC-O, AC-B, and AC-A are 0.007, 0.006, 0.009, 0.006, and 0.010 g/(h·mg), respectively.

However, it is widely acknowledged that the pseudo-second-order model can hardly identify the diffusion process of the adsorption. Hence, the intra-particle diffusion model is applied [29]. The model is shown as following:

$$q_t = k_p t^{1/2} + C \tag{12}$$

In this equation, q_t is the amount of bromate adsorbed at time t (mg/g), k_p is the intra-particle diffusion rate constant (mg/($h^{1/2}$·g)), and C is the intercept.

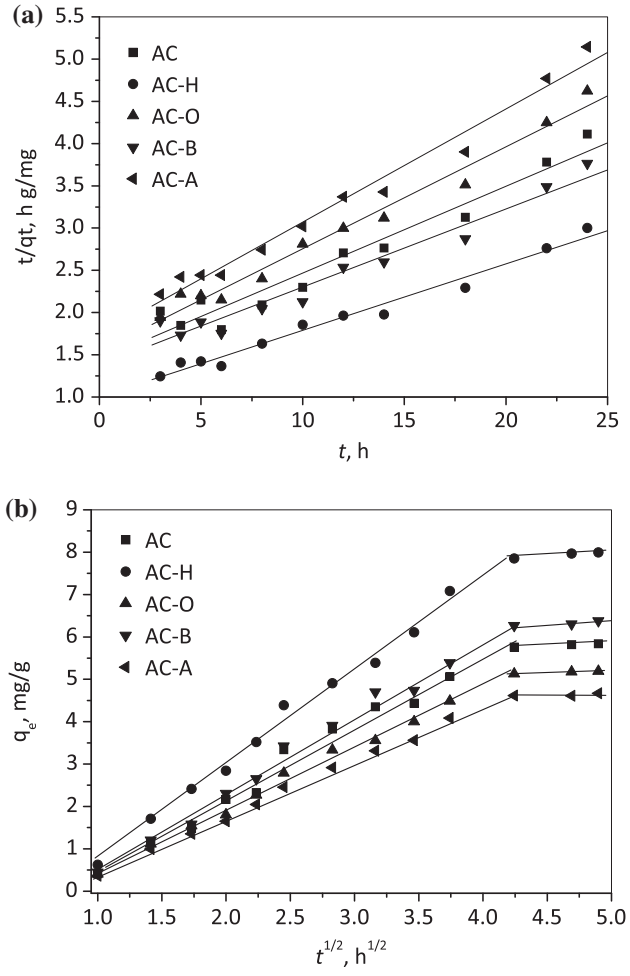

Fig. 2. Application of the pseudo-second-order and intra-particle diffusion model to the experimental kinetic data for bromate adsorption ((a) pseudo-second-order model; (b) intra-particle diffusion model).

Fig. 2(b) shows the fitting process of the intra-particle diffusion model with the experimental data. The high values of the coefficient ($R^2 > 0.98$) indicate that the process of bromate adsorption by the ACs are better fitted by the intra-particle diffusion model than the pseudo-second-order model. The intra-particle diffusion rate constants of the AC, AC-H, AC-O, AC-B, and AC-A are 1.69, 2.23, 1.45, 1.82, and 1.32 mg/$h^{1/2}$·g, respectively.

Previous studies have reported that the process of the adsorption can generally be broken down into two or more steps [29]. Commonly, the first sharper portion shown in the figure is classified as the external surface adsorption or instantaneous adsorption stage. The second step is regarded as the gradual adsorption process. In this stage, the intra-particle diffusion is rate limited. The third step is the final equilibrium step. In the final equilibrium step, under the effect of the lowered concentration of sorbate in the solution, the intra-particle diffusion slows down. The fitting results shown in the figure indicate that the two-stage adsorption process occurs in bromate adsorption. The first linear portion of the plot is the stage of surface adsorption. This stage is generally ascribed to the boundary layer effect. The second linear portion, which is aroused by the intraparticle/pore diffusion within the pores of the ACs, is the intra-particle diffusion stage. In addition, the results shown in the figure reveal that for all of the ACs, the intra-particle diffusion commonly applies during the initial 16 h of the adsorption. These results reveal that the intra-particle diffusion controls the limiting rate of the bromate adsorption on the ACs.

3.3. Adsorption isotherms

Adsorption isotherm experiments were conducted to reveal the maximum bromate adsorption capacities of the AC samples. The data obtained at 298 K are shown in Fig. 3. From the diagram, it is seen that the bromate uptake increases gradually with the equilibrium concentration increasing. Two isotherms equations including Freundlich and Langmuir [29,30], described in Eqs. (13) and (14), are applied to fit the experimental data.

Table 3
Rate constant and correlation coefficients for the kinetic models

	Pseudo-second-order parameters			Intra-particle diffusion parameters	
	k (g/(h·mg))	q_e (mg/g)	R^2	k_p, (mg/$h^{1/2}$·g)	R^2
AC	0.007	9.73	0.951	1.69	0.984
AC-H	0.006	12.7	0.982	2.23	0.994
AC-O	0.009	8.29	0.982	1.45	0.995
AC-B	0.006	10.8	0.961	1.82	0.991
AC-A	0.010	7.47	0.983	1.32	0.997

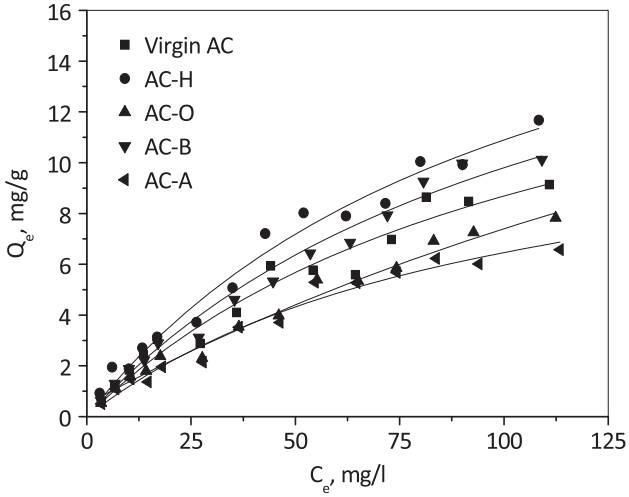

Fig. 3. Isotherms of bromate adsorption for different ACs at 298 K.

$$\text{Langmuir equation: } \left(q_e = \frac{q_m b C_e}{1 + bC_e}\right) \quad (13)$$

$$\text{Freundlich equation: } \left(q_e = KC_e^{1/n}\right) \quad (14)$$

In these equations, C_e and q_e are the solution concentration (mg/l) and the adsorbed amount (mg/g) of bromate at equilibrium. The other parameters are the constants of the isotherm models. These constants can be acquired by regression of the isotherm data.

The estimated model parameters are shown in Table 4. It can be seen from the table that the date are well fitted by these two models. In term of R^2, the Freundlich equation isotherm model provides a better fitting than the Langmuir equation.

The estimated model parameters, which are shown in Table 4, provide comprehensive comparison of the capacities of these ACs in bromate adsorption. Specially, the values of the parameter q_m in Langmuir equation represents the maximum capacity of the AC sample in bromate removal. From the Table, it can be seen that the maximum adsorption capacity of the virgin AC in bromate uptake is about 18.5 mg/g.

The thermal modification process is found to have great benefit for the adsorption capacity and the q_m of the AC-H is about 22.5 mg/g, which is a 22% increase. The HNO_3 modification process brings a dramatic decrease of the adsorption capacity and the q_m of the AC-A is 11.9 mg/g. It is also found that the alkaline modification process increases the adsorption capacity and the q_m of the AC-B is about 20.3 mg/g, about 1.1 times of that of the virgin AC. The H_2O_2 modification process decreases the maximum adsorption capacity slightly and the q_m of the AC-O is about 17.3 mg/g.

For an insight into the mechanism of bromate adsorption, efforts were done to reveal the relationship between the surface properties and the maximum adsorption capacity. Fig. 4 shows the correlation between the maximum adsorption capacities and the percentage of the acidic groups in total groups. It can be seen that the maximum adsorption capacity yields a correlation of 86.3% with the ratio, indicating that the adsorption capacity for bromate adsorption is strongly dependent on the content of the acidic groups on AC surface. In brief, the more the acidic groups found on the AC surface, the lower the adsorption capacity of the AC.

It is reported that in aqueous solutions, increase of the amount of acidic groups on the surface promotes

Table 4
Experimental equilibrium adsorption data of the samples

Freundlich equation $q_e = KC_e^{1/n}$			
	K	n	R^2
AC	0.37	1.45	0.965
AC-H	0.47	1.45	0.979
AC-O	0.29	1.48	0.962
AC-B	0.42	1.45	0.983
AC-A	0.25	1.37	0.985
Langmuir equation $q_e = \frac{q_m b C_e}{1+bC_e}$			
	q_m	b	R^2
AC	18.5	0.009	0.961
AC-H	22.5	0.009	0.979
AC-O	17.3	0.011	0.973
AC-B	20.3	0.009	0.978
AC-A	11.9	0.012	0.972

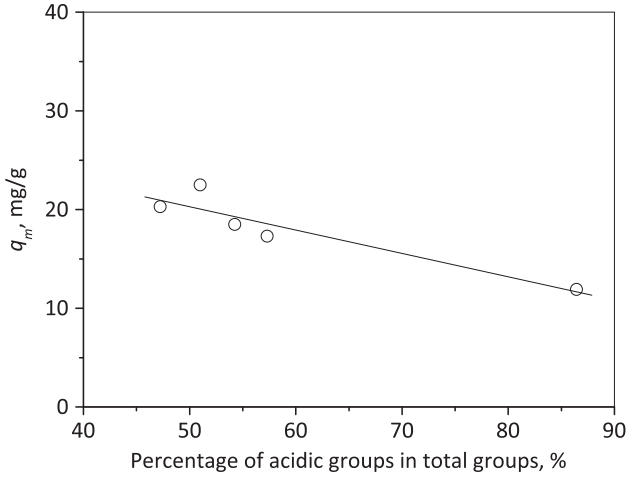

Fig. 4. Correlation of q_m with the percentage of acidic groups in total groups.

the formation of water clusters and the removal of π electrons from the basal planes [31,32]. Under this condition, the interactions between the AC surface and the ionic substances are weakened. Besides, the presence of the carboxylic groups would bring a decrease of the pH_{PZC}, which makes the surface of the AC negatively charged. The ACs with lower acidic groups is less negatively charged under the same pH condition. So, the repulsion between the AC surface and the dissolved BrO_3^- anions is reduced, and higher adsorption capacity can be obtained for the AC-H and AC-B. In addition, it can be seen from the results of AC texture characterization that the HNO_3 modification and H_2O_2 modification processes not only produced carboxylic groups on AC surface, but also brought a significant decrease of the surface area. The reduced specific surface area of the sample AC-O and AC-A weakened the contact opportunities for anions with AC surface. Therefore, based on the above analysis, the amount of the bromate adsorbed by AC-A (acidic groups in total groups = 86.42%) is markedly lower than the amounts adsorbed by the heat-treated and alkaline-treated ACs (acidic groups in total groups = 51.0 and 47.2%, respectively).

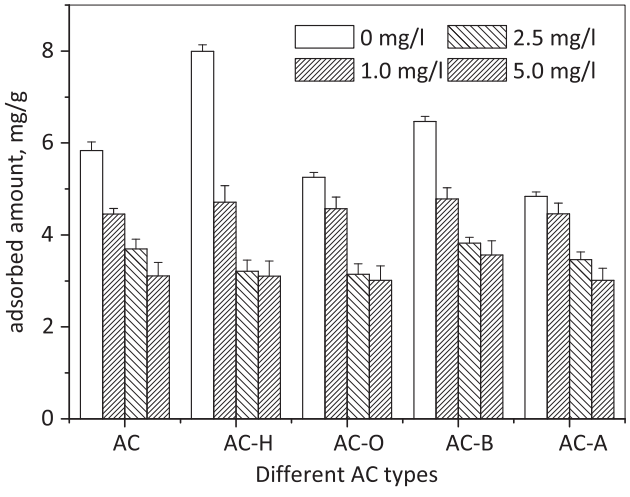

Fig. 5. Effect of NOM concentrations on bromate uptake.

3.4. Effect of NOM and anions

Fig. 5 shows the bromate uptake for different ACs in the presence of natural organic matters (NOM). In this case, humic acid was dissolved in water to simulate the NOM substance in water. From the diagram, it can be seen that the presence of NOM showed a negative effect on the bromate uptake, which dovetails nicely with previous studies. Previous studies showed that the presence of NOM in water can block active sites of ACs, and decrease the bromate adsorption capability of a carbon. Mills et al. [33] conducted bromate adsorption under two natural waters with different DOC, Cl^-, and SO_4^{2-} concentrations, and found that more bromate can be removed in the water with lower DOC and anion concentrations. Bao et al. [3] investigated the effects of NOM, bromide, nitrate, and sulfate on bromate adsorption, and found that these constituents hastened bromate breakthrough in GAC filter. Though all of the tested ACs present a significant decrease of adsorbility under the pressure of the NOM, AC-H and AC-B lose more adsorbility under the same NOM concentrations than the samples AC-O and AC-A. For virgin AC, the bromate uptake under the NOM concentrations of 1, 2.5, and 5 mg/l NOM are 4.5, 3.7, and 3.1 mg/g, which are 76.3, 63.3, and 53.2% of the uptake without NOM. The uptake of AC-H under NOM pressure are 58.9, 40.2, and 38.8%, while the uptake of AC-A are 92.2, 71.5, and 62.2%, showing that the AC-H are tend to be more affected by the NOM in adsorption of bromate. This can be ascribed to both the molecular form of the NOM and the charge of the AC surface. The test was operated at neutral pH condition (pH = 6.0), the functional groups such as –COOH and –COH of the NOM tended to be dissociated to ionic species, and thus, the hydrophilicity of the NOM was increased. Also, the surface of the ACs with lower pH_{pzc} (AC-O and AC-A) tends to be negatively charged. Due to the electrostatic repulsions between the NOM and the negatively charged AC surface, NOM can hardly be adsorbed [29] and reduced, so the AC-A and AC-O is not as sensitive as AC-H and AC-B, when NOM is presented.

Fig. 6 shows the bromate uptake for AC-H in the individual presence of nitrate, sulfate, and chloride. The uptake data are presented as a function of the

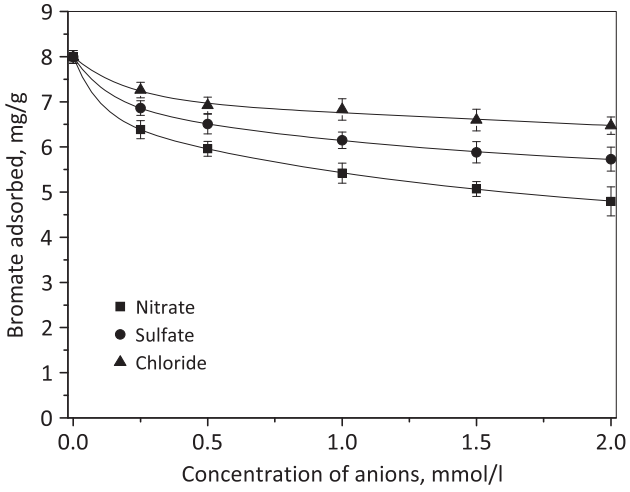

Fig. 6. Effect of anion concentrations on bromate uptake for AC-H.

starting concentration of the anions. In each case, the presence of the anions could reduce the amount of the bromate adsorbed on AC-H to some extent. It can be seen from the figure that, with the increase of the initial concentration of anions, the amount of the bromate absorbed decreased. When the concentrations of nitrate, sulfate, and chloride were increased from 0 to 2.0 mmol/l, the bromate uptake decreased from 8.0 (with bromate only) to 4.8, 5.7, and 6.5 mg/g, respectively.

It is commonly regarded that the process of the bromate removal by AC composed of the stages of adsorbed onto surface, reduced to hypobromite (BrO^-) and finally reduced to bromide. The Cl^-, SO_4^{2-} or (NO_3^- anions can also be removed by AC through the effect of ion exchange. The Cl^-, SO_4^{2-} or (NO_3^- anions presented in water may compete with bromate for exchange sites on AC surface. When the concentrations of nitrate, chloride, and sulfate increase, more competitions for bromate reduction sites are found, resulting in limited available active site and lowered bromate uptake. The competitive effect was greatest for nitrate, followed by sulfate and chloride at the same concentration, indicating that the selectivity order of bromate anion over other anions on the AC-H was $(NO_3^- > SO_4^{2-} > Cl^-$.

4. Conclusions

This study examined bromate adsorption by using four types of modified ACs. The results show that the thermal and alkaline modified ACs, with lower amount of acidic functional groups on surface, present higher capacities in bromate adsorption. Comparative study of the adsorption capacities and the surface functional groups indicate that there is a remarkable linear relation between the adsorption capacity and the content of the acidic groups in total groups. The carbon with lower acidic surface groups and higher pH_{PZC} has higher bromate adsorption capacity, while the carbon with higher acidic groups and lower pH_{PZC} groups has lower capacity. The presence of the other anions ((NO_3^-, SO_4^{2-}, Cl^-) could reduce the amount of bromate adsorbed on the AC-H. However, the AC-H exhibited a high bromate selectivity for these competitive anions and the selectivity order was $((NO_3^- > SO_4^{2-} > Cl^-$. The presence of NOM showed a negative effect, since it can block active sites of ACs. However, the AC-A and AC-O are not as sensitive as AC-H and AC-B, when NOM is presented.

Acknowledgments

The authors would like to acknowledge the financial support for this work provided by Chongqing University and the Tianjin Key Laboratory of Aquatic Science and Technology.

References

[1] B. Legube, B. Parinet, K. Gelinet, F. Berne, J.P. Croue, Modeling of bromate formation by ozonation of surface waters in drinking water treatment, Water Res. 38 (2004) 2185–2195.
[2] M.S. Siddiqui, G.L. Amy, R.G. Rice, Bromate ion formation – A critical-review, J. AWWA 87 (1995) 58–70.
[3] M.L. Bao, O. Griffini, D. Santianni, K. Barbieri, D. Burrini, F. Pantani, Removal of bromate ion from water using granular activated carbon, Water Res. 33 (1999) 2959–2970.
[4] P. Westerhoff, Reduction of nitrate, bromate, and chlorate by zero valent iron (Fe-0), J. Environ. Eng. Asce. 129 (2003) 10–16.
[5] L. Xie, C. Shang, The effects of operational parameters and common anions on the reactivity of zero-valent iron in bromate reduction, Chemosphere 66 (2007) 1652–1659.
[6] R. Chitrakar, A. Sonoda, Y. Makita, T. Hirotsu, Synthesis and bromate reduction of sulfate intercalated Fe(II)–Al(III) layered double hydroxides, Sep. Purif. Technol. 80 (2011) 652–657.
[7] R. Chitrakar, Y. Makita, A. Sonoda, T. Hirotsu, Fe-Al layered double hydroxides in bromate reduction: Synthesis and reactivity, J. Colloid Interface Sci. 354 (2011) 798–803.
[8] E. Agus, N. Voutchkov, D.L. Sedlak, Disinfection by-products and their potential impact on the quality of water produced by desalination systems: A literature review, Desalination 237 (2009) 214–237.
[9] S. Gyparakis, E. Diamadopoulos, Formation and reverse osmosis removal of bromate ions during ozonation of groundwater in coastal areas, Sep. Sci. Technol. 42 (2007) 1465–1476.
[10] R. Song, R. Minear, P. Westerhoff, G. Amy, Bromate formation and control during water ozonation, Environ. Technol. 17 (1996) 861–868.
[11] A.H. Konsowa, Bromate removal from water using granular activated carbon in a batch recycle, Desalin. and Water Treat. 12 (2009) 375–381.
[12] C.T. Matos, S. Velizarov, M.A. Reis, J.G. Crespo, Removal of bromate from drinking water using the ion exchange membrane bioreactor concept, Environ. Sci. Technol. 42 (2008) 7702–7708.

[13] X. Huang, N.Y. Gao, Y. Deng, Bromate ion formation in dark chlorination and ultraviolet/chlorination processes for bromide-containing water, J. Environ. Sci. China 20 (2008) 246–251.
[14] S. Peldszus, S.A. Andrews, R. Souza, F. Smith, I. Douglas, J. Bolton, P.M. Huck, Effect of medium-pressure UV irradiation on bromate concentrations in drinking water, a pilot-scale study, Water Res. 38 (2004) 211–217.
[15] M.S. Siddiqui, G.L. Amy, L.J. McCollum, Bromate destruction by UV irradiation and electric arc discharge, Ozone Sci. Eng. 18 (1996) 271–290.
[16] L.A. Wang, J. Zhang, J.Z. Liu, H. He, M. Yang, J.W. Yu, Z.C. Ma, F. Jiang, Removal of bromate ion using powdered activated carbon, J. Environ. Sci. China 22 (2010) 1846–1853.
[17] W.J. Huang, Y.L. Cheng, Effect of characteristics of activated carbon on removal of bromate, Sep. Purif. Technol. 59 (2008) 101–107.
[18] A. Bhatnagar, M. Sillanpaa, Sorption studies of bromate removal from water by Nano-Al_2O_3, Sep. Sci. Technol. 47 (2012) 89–95.
[19] Y. Cui, Z. Hu, J. Chen, Removal of bromate from aqueous solution by corncobs, Desalin. and Water Treat. 28 (2011) 338–344.
[20] W.J. Huang, C.Y. Chen, M.Y. Peng, Adsorption/reduction of bromate from drinking water using GAC: Effects on carbon characteristics and long-term pilot study, Water Sa. 30 (2004) 369–375.
[21] M.J. Kirisits, V.L. Snoeyink, J.P. Kruithof, The reduction of bromate by granular activated carbon, Water Res. 34 (2000) 4250–4260.
[22] M. Siddiqui, W.Y. Zhai, G. Amy, C. Mysore, Bromate ion removal by activated carbon, Water Res. 30 (1996) 1651–1660.
[23] M. Asami, T. Aizawa, T. Morioka, W. Nishijima, A. Tabata, Y. Magara, Bromate removal during transition from new granular activated carbon (GAC) to biological activated carbon (BAC), Water Res. 33 (1999) 2797–2804.
[24] H.L. Chiang, C.P. Huang, P.C. Chiang, The surface characteristics of activated carbon as affected by ozone and alkaline treatment, Chem. 47 (2002) 257–265.
[25] J. Rivera-Utrilla, M. Sanchez-Polo, V. Gomez-Serrano, P.M. Alvarez, M.C.M. Alvim-Ferraz, J.M. Dias, Activated carbon modifications to enhance its water treatment applications, J. Hazard. Mater. 187 (2011) 1–23.
[26] J.S. Noh, J.A. Schwarz, Estimation of the point of zero charge of simple oxides by mass titration, J. Colloid Interf. Sci. 130 (1989) 157–164.
[27] H.P. Boehm, M. Voll, Basic surface oxides on carbon.1. adsorption of acids, Carbon 8 (1970) 227–240.
[28] C.Y. Yin, M.K. Aroua, W.M. Daud, Review of modifications of activated carbon for enhancing contaminant uptakes from aqueous solutions, Sep. Purif. Technol. 52 (2007) 403–415.
[29] L.C. Lei, X.J. Li, X.W. Zhang, Ammonium removal from aqueous solutions using microwave-treated natural Chinese zeolite, Sep. Purif. Technol. 58 (2008) 359–366.
[30] L. Gu, X.W. Zhang, L.C. Lei, Y. Zhang, Enhanced degradation of nitrophenol in ozonation integrated plasma modified activated carbons, Micropor. Mesopor. Mater. 119 (2009) 237–244.
[31] I.I. Salame, T.J. Bandosz, Role of surface chemistry in adsorption of phenol on activated carbons, J. Colloid Interf. Sci. 264 (2003) 307–312.
[32] G. Skodras, I. Diamantopoujou, G.P. Sakellaropoujos, Role of activated carbon structural properties and surface chemistry in mercury adsorption, Desalination 210 (2007) 281–286.
[33] A. Mills, A. Belghazi, D. Rodman, P. Hitchins, The removal of bromate from potable water using granular activated carbon, J. Ins. Water Environ. Manag. 10 (1996) 215–217.